

Bayesian Multi-Subject Factor Analysis to Predict Microsleeps from EEG Power Spectral Features

Reza Shoorangiz, *Student Member, IEEE*, Stephen J. Weddell, *Senior Member, IEEE*,
Richard D. Jones, *Fellow, IEEE*

Abstract—Prediction of an imminent microsleep has the potential to save lives and prevent catastrophic accidents. A microsleep is a brief episode of unintentional unconsciousness and, hence, loss of responsiveness. In this study, prediction of imminent microsleeps using EEG data from 8 subjects was examined. A novel Bayesian algorithm was proposed to identify common components of pre-microsleep activity in the EEG in all subjects and predict microsleeps 0.25 s ahead. To avoid overfitting, this model incorporates sparsity-promoting priors to automatically find the minimum number of components. Due to intractability of full Bayesian treatment, variational Bayesian was integrated to approximate posterior probabilities. To predict microsleeps, EEG log-power spectral features were extracted from a 5-s window. Bayesian multi-subject factor analysis was used to extract common microsleep patterns and transform all features into lower-dimension common-space features. Discrimination between responsive and microsleep instances was done with a single linear discriminant analysis (LDA) classifier. Performance of the proposed method was evaluated using leave-one-subject-out cross-validation. Our prediction system achieved moderate AUC_{ROC} and GM of 0.90 and 0.80, respectively, but with a relatively low precision of 0.29.

I. INTRODUCTION

A brief unintentional episode of sleep-related suspension of performance from 0.5–15 s, i.e., a microsleep, while performing an active and monotonous task, such as driving, is a safety threat, which can lead to catastrophic consequences [1]. Tefft [2] estimated that drowsy drivers were involved in 13% of car crashes resulting in hospitalization, and 21% of fatal car crashes in the USA. Fatigue was also involved in 16% of fatal crashes in New South Wales [3]. A National Sleep Foundation survey in the USA showed that 65% of participated drivers had experienced drowsiness behind the wheel in the past year, while more than one-third acknowledged falling asleep while driving [4]. Similarly, more than half (58%) of participants in a public poll in Ontario admitted experiencing drowsiness and 14% acknowledged

falling asleep while driving [5]. These studies indicate that drowsiness and fatigue are substantial contributing factors to car accidents.

Microsleeps can occur frequently even in non-sleep-deprived healthy people. Peiris et al. [6] found an average rate of $15.2 (0.0\text{--}72.0)h^{-1}$ microsleeps in 15 participants performing a 1-D continuous task. Similarly, Poudel et al. [7] reported an average rate of microsleeps of $79h^{-1}$, with a mean duration of 3.3 s, while non-sleep-deprived participants performed a 2-D tracking task in an MRI-scanner for 50 min. Moreover, Sirois et al. [8] found a high correlation between microsleep duration and accident event probability. These indicate the importance of early detection and even prediction of microsleeps, so that a wake-up alarm can be sounded and a fatal accident averted.

Lal and Craig [9] showed that spectral components of EEG have high reproducibility among fatigued drivers. Wang et al. [10] used EEG power spectra to detect fatigue and lapse. Peiris et al. [11] analysed EEG power spectral and other nonlinear features, such as fractal dimension, approximate entropy, and Lempel-Ziv complexity, for microsleep detection. They found spectral features had the highest detection performance among other features. Davidson et al. [12] used a long-short-term-memory (LSTM) recurrent neural network to capture temporal dynamics of EEG power spectral features to detect microsleeps. Lastly, our preliminary analysis also showed that power spectral features of EEG contained information predictive of microsleeps [13].

In this study, our aim was to improve the performance of microsleep prediction by incorporating subject-variability into a feature reduction model. To this end, a Bayesian multi-subject factor analysis model was proposed. Due to intractability of full Bayesian treatment, variational inference was applied to approximate posterior probability distributions. Leave-one-subject-out cross-validation was employed to measure performance of the proposed method [12].

II. METHODOLOGY

A. Data

This study included 15 healthy participants, who had reported an average previous night's sleep of 7.8 ± 1.2 h. Participants had no neurological or sleep disorders [6]. The task was based on 1-D random preview tracking in which participants were asked to follow a moving cursor as accurately as possible using a steering wheel. Scalp EEG was recorded from 16 channels, namely, Fp1, Fp2, F3, F4, F7, F8, C3, C4, O1, O2, P3, P4, T3, T4, T5, and T6,

* This work was supported by the University of Canterbury and the New Zealand Brain Research Institute.

Reza Shoorangiz is with the Department of Electrical and Computer Engineering at University of Canterbury, Christchurch Neurotechnology Research Programme, and New Zealand Brain Research Institute, Christchurch, New Zealand (email: reza.shoorangiz@nzbrri.org).

Stephen Weddell is with the Department of Electrical and Computer Engineering at University of Canterbury and Christchurch Neurotechnology Research Programme, Christchurch, New Zealand (email: steve.weddell@canterbury.ac.nz).

Richard Jones is with the Department of Electrical and Computer Engineering at University of Canterbury, Christchurch Neurotechnology Research Programme, and New Zealand Brain Research Institute, Christchurch, New Zealand (email: richard.jones@nzbrri.org).

placed according to the international 10-20 system. EEG was sampled at 256 Hz. Tracking data and facial video were also recorded to identify microsleeps through behavioural cues. Each participant performed two 1 h sessions.

B. EEG Preprocessing

EEG data were filtered using a band-pass finite impulse response with cut-off frequencies of 1 Hz and 45 Hz. Next, a moving artefact subspace reconstruction (ASR) [13], [14] with 2-min window length and 50% overlap was used to remove artefacts with a z-score over 5. Lastly, canonical correlation analysis blind source separation [15] was applied to remove muscle artefacts.

C. Microsleeps and Gold-standard

Microsleeps were identified from recorded facial video and tracking performance. An expert independently examined facial video recordings to identify behavioural clues using a 6-scale rating, i.e., alert, distracted, forced eye closure, light drowsy, deep drowsy, and microsleep [6], [11]. In parallel, tracking performance was analysed to find ‘responsive’, ‘deviated’, and ‘flat-spot’ regions [13]. Lastly, video and tracking analyses were used to generate the final gold-standard as follows:

- ‘responsive’: subject is closely tracking the target, irrespective of video rating,
- ‘microsleep’: subject is not tracking the target, and the video rating is deep drowsy or microsleep,
- ‘uncertain’: remainder of data which is not explained by ‘responsive’ or ‘microsleep’.

D. Feature extraction

EEG data was segmented into 5-s windows, in which each segment corresponded to a gold-standard τ ahead, as shown in Fig. 1. In this study, τ was set to 0.25-s and the gold-standard frequency was 4 Hz. Power density of various EEG frequency bands were then estimated for each channel using Welch’s method with 2-s windows and 75% overlap. These frequency bands were delta (1–4.5 Hz), theta (4.5–8 Hz), alpha1 (8–10.5 Hz), alpha2 (10.5–12.5 Hz), alpha (8–12.5 Hz), beta1 (12.5–15 Hz), beta2 (15–25 Hz), beta (12.5–25 Hz), gamma1 (25–35 Hz), gamma2 (35–45 Hz), gamma (25–45 Hz), and overall (1–45 Hz). A total of 192 features were extracted and all estimated powers were transformed into log-space.

E. Bayesian Multi-Subject Factor Analysis

We assume that S subjects share a set of latent components while they experience microsleeps. Each subject has N_s independently and identically distributed microsleep observations where $s \in 1, \dots, S$. This can be formulated as:

$$\mathbf{x}_{s,n} \sim \mathcal{N}(\boldsymbol{\mu}_s + \mathbf{W}\mathbf{z}_{s,n}, \boldsymbol{\Psi}_s^{-1}), \quad (1)$$

where $\mathcal{N}(\boldsymbol{\mu}, \boldsymbol{\Sigma})$ represents a multivariate normal distribution with mean $\boldsymbol{\mu}$ and covariance matrix $\boldsymbol{\Sigma}$, \mathbf{x} is a D -dimensional feature vector, \mathbf{z} is a K -dimensional vector of latent variable, \mathbf{W} is a $D \times K$ loading matrix, and $\boldsymbol{\Psi}$ is a precision matrix.

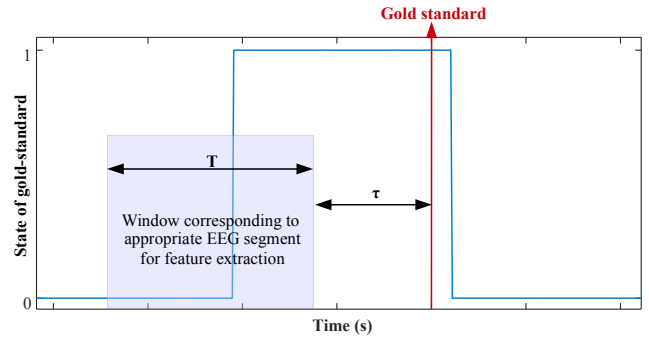


Fig. 1. Association between EEG segment and gold-standard.

A zero mean normal distribution was assigned as the prior distribution of the latent variable,

$$\mathbf{z} \sim \mathcal{N}(\mathbf{0}, \mathbf{I}_K). \quad (2)$$

Prior distributions of parameters $\boldsymbol{\mu}_s$ and $\boldsymbol{\Psi}_s$ are given as

$$p(\boldsymbol{\mu}_s | \boldsymbol{\Psi}_s) = \prod_{d=1}^D \mathcal{N}(\mu_{s,d} | 0, (\beta_0 \psi_{s,d})^{-1}), \quad (3)$$

$$p(\boldsymbol{\Psi}_s) = \prod_{d=1}^D \mathcal{G}(\psi_{s,d} | a_\psi, b_\psi), \quad (4)$$

where $\mathcal{G}(a, b)$ is Gamma distribution given by

$$\mathcal{G}(x | a, b) = \frac{1}{\Gamma(a)} b^a x^{a-1} \exp(-bx), \quad (5)$$

and β_0 , a_ψ , and b_ψ are hyperparameters and shared among all the subjects. Each column of \mathbf{W} corresponds to a component of latent variables. A hierarchical prior utilizing automatic relevance determination (ARD) was used over loading matrix \mathbf{W} such that

$$p(\mathbf{W} | \boldsymbol{\alpha}) = \prod_{k=1}^K \mathcal{N}(\mathbf{w}_k | \mathbf{0}, \alpha_k^{-1} \mathbf{I}), \quad (6)$$

$$p(\boldsymbol{\alpha}) = \prod_{k=1}^K \mathcal{G}(\alpha_k | a_\alpha, b_\alpha), \quad (7)$$

where \mathbf{w}_k is the k^{th} column of \mathbf{W} , and a_α and b_α are hyperparameters. The precision of the k^{th} column of loading matrix \mathbf{W} is controlled by α_k . Therefore, the concentration of posterior distribution of α_k on large values will result in \mathbf{w}_k having values closer to zero. This effectively identifies the number of factors and removes unnecessary components [16]. A probabilistic graphical model of multi-subject factor analysis is shown in Fig. 2.

We performed variational Bayesian inference [17] to approximate posterior distributions, since fully Bayesian treatment of multi-subject factor analysis is intractable. The goal of variational inference is to maximize the lower bound of the evidence $\mathcal{L}(q)$,

$$\begin{aligned} \ln(p(\mathbf{X})) &= \ln\left(\int p(\mathbf{X}, \boldsymbol{\theta}) d\boldsymbol{\theta}\right) \\ &\geq \int q(\boldsymbol{\theta}) \ln\left(\frac{p(\mathbf{X}, \boldsymbol{\theta})}{q(\boldsymbol{\theta})}\right) d\boldsymbol{\theta} = \mathcal{L}(q), \end{aligned} \quad (8)$$

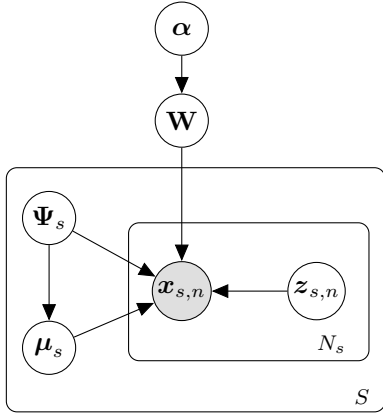


Fig. 2. Probabilistic graphical model representation of multi-subject Bayesian factor analysis.

where $\theta = \{\theta_i\}$ denotes all the latent variables, parameters, and hyperparameters, and $q(\theta)$ is the approximating distribution.

In order to perform variational analysis, we assume $q(\theta)$ is factorized as

$$q(\mathbf{Z}, \mathbf{W}, \alpha, \mu, \Psi) = q(\mathbf{Z}) q(\mathbf{W}) q(\alpha) q(\mu, \Psi). \quad (9)$$

The expressions for approximating distributions are

$$q(\mathbf{Z}) = \prod_{s=1}^S \prod_{n=1}^{N_s} \mathcal{N}(z_{s,n} | \tilde{\mathbf{m}}_{z,n}^s, \tilde{\Sigma}_z^s), \quad (10)$$

$$q(\mathbf{W}) = \prod_{d=1}^D \mathcal{N}(\hat{\mathbf{w}}_d | \tilde{\mathbf{m}}_{w,d}, \tilde{\Sigma}_{w,d}), \quad (11)$$

$$q(\alpha) = \prod_{k=1}^K \mathcal{G}(\alpha_k | \tilde{a}_{\alpha}, \tilde{b}_{\alpha,k}), \quad (12)$$

$$q(\mu | \Psi) = \prod_{s=1}^S \prod_{d=1}^D \mathcal{N}(\mu_{s,d} | \tilde{\mathbf{m}}_{\mu,d}^s, (\beta_{\mu}^s \psi_d^s)^{-1}), \quad (13)$$

$$q(\Psi) = \prod_{s=1}^S \prod_{d=1}^D \mathcal{G}(\psi_{s,d} | \tilde{a}_{\psi}^s, \tilde{b}_{\psi,d}^s), \quad (14)$$

where

$$\tilde{\Sigma}_z^s = (\langle \mathbf{W}^{\top} \Psi_s \mathbf{W} \rangle + \mathbf{I})^{-1},$$

$$\tilde{\mathbf{m}}_{z,n}^s = \tilde{\Sigma}_z^s \langle \mathbf{W}^{\top} \rangle (\langle \Psi_s \rangle \mathbf{x}_{s,n} - \langle \Psi_s \mu_s \rangle),$$

$$\beta_{\mu}^s = N_s + \beta_0,$$

$$\tilde{\mathbf{m}}_{\mu,d}^s = \frac{1}{\beta_{\mu}^s} \sum_{n=1}^{N_s} (x_{n,d}^s - \langle \hat{\mathbf{w}}_d^{\top} \rangle \langle z_{s,n} \rangle),$$

$$\tilde{\Sigma}_{w,d} = \left(\langle \text{diag}(\alpha) \rangle + \sum_{s=1}^S \langle \psi_{s,d} \rangle \sum_{n=1}^{N_s} \langle z_{s,n} z_{s,n}^{\top} \rangle \right)^{-1},$$

$$\tilde{\mathbf{m}}_{w,d} = \tilde{\Sigma}_{w,d} \sum_{s=1}^S \langle \psi_{s,d} \rangle \sum_{n=1}^{N_s} (\langle z_{s,n} \rangle (x_{s,n}^d - \langle \mu_{s,d} \rangle)),$$

$$\tilde{a}_{\alpha} = a_{\alpha} + \frac{D}{2},$$

$$\tilde{b}_{\alpha,k} = b_{\alpha} + \frac{\langle \mathbf{w}_k^{\top} \mathbf{w}_k \rangle}{2},$$

$$\begin{aligned} \tilde{a}_{\psi}^s &= a_{\psi} + \frac{N_s}{2}, \\ \tilde{b}_{\psi,d}^s &= b_{\psi} - \frac{\beta_{\mu}^s}{2} \tilde{\mathbf{m}}_{\mu,d}^s{}^2 \\ &\quad + \frac{1}{2} \sum_{n=1}^{N_s} \left(x_{s,n}^d{}^2 - 2x_{s,n}^d \langle \hat{\mathbf{w}}_d^{\top} \rangle \langle z_{s,n} \rangle \right. \\ &\quad \left. + \text{tr} \left(\langle \hat{\mathbf{w}}_d \hat{\mathbf{w}}_d^{\top} \rangle \langle z_{s,n} z_{s,n}^{\top} \rangle \right) \right). \end{aligned}$$

It is notable that $\hat{\mathbf{w}}_d^{\top}$ corresponds to the d^{th} row of loading matrix \mathbf{W} , $\langle \cdot \rangle$ denotes expectation with respect to $q(\theta)$, and $\text{diag}(\alpha)$ denotes a matrix with $\{\alpha_k\}$ as diagonal elements. A numerical solution of approximate distributions can be found by iterating over variables and updating one at a time. Lower bound $\mathcal{L}(q)$ can then be used to monitor convergence.

F. Classification

We included only those subjects who had had at least one microsleep whilst performing the tracking task outlined in Section II.A ($N = 8$). To measure performance of our system, one subject was left out as test data while data of the other 7 subjects were used to train the prediction model. This process was repeated 8 times and test performances were averaged.

For each test, a Bayesian multi-subject factor analysis was applied to the microsleep portion of the training data to find the posterior probability of a common loading matrix, given microsleep data of all seven training subjects. Latent features were then inferred by fixing the probability distribution of the loading matrix to the posterior from previous step, and inferring μ and Ψ for each subject. An LDA classifier was employed to discriminate between microsleep and responsive using latent features. Batch learning was performed for training data, but online inference was employed for test data. To this end, our variational Bayesian model was first initialized to the first 60s of data, and then updated every 2s.

To evaluate performance of our system, multiple measures were used including area under the curve of receiver operating characteristic (AUC_{ROC}), area under the curve of precision-recall (AUC_{PR}), geometric mean (GM), phi correlation coefficient (φ), sensitivity, specificity, and precision.

III. RESULTS

Bayesian multi-subject factor analysis let the training data share information, while having individual variations. Each common component consists of a linear combination of 12 log-powers of various frequency bands within 16 channels. Fig. 3 is a topographic scalp map representing spatial distribution of a common component extracted from 7 training subjects. This component showed a mixture of activities in left temporal in Delta and Beta1 bands, and frontal areas in Gamma band.

The average values of performance of the 8 test subjects were: $\text{AUC}_{\text{ROC}} = 0.90$, $\text{AUC}_{\text{PR}} = 0.36$, sensitivity = 0.72, specificity = 0.89, $\varphi = 0.34$, GM = 0.80, and precision = 0.29. Due to a highly variable imbalance ratio (IR) among

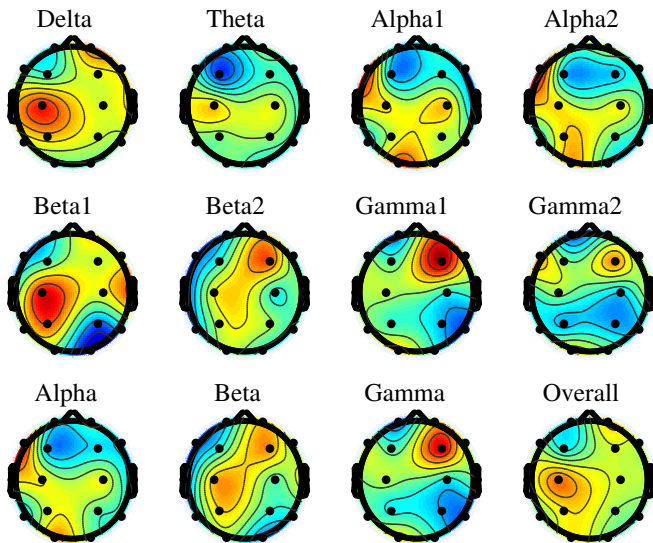


Fig. 3. A topographic representation of spatial weights of a common component for log-power of different frequency bands.

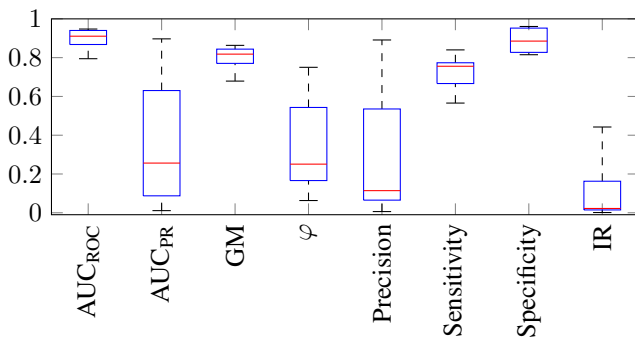


Fig. 4. Distribution of performance measures and imbalance ratios over 8 independent test subjects.

the test subjects, the precision values were widespread (0.01–0.89). AUC_{PR} and φ also spanned a wide range of values, i.e., 0.09–0.90 and 0.06–0.75, respectively. On the other hand, AUC_{ROC} and GM were less influenced by IR. The distributions of various performance measures, as well as IR, are shown in Fig. 4.

IV. DISCUSSION

Continuous prediction of 0.25 s ahead microsleep or responsive state was investigated in this study. We applied Bayesian multi-subject factor analysis to extract common space microsleep features among all training subjects, where features were log-power spectral of various frequency bands. In addition, test data were applied in an online and adaptive fashion, where the first 60 s was used to initialize parameters of Bayesian model, and then it was updated every 2 s. Leave-one-subject-out cross-validation was used to evaluate the performance of our proposed method, and average values of different measures were reported.

Comparing the performance of this model with our previous work [13] shows that average GM and φ were slightly improved, i.e., 0.80 vs 0.74 and 0.34 vs 0.33, respectively, while AUC_{ROC} remained the same (0.90). Moreover, the

average number of retained components in this study was 115, while 37–40 features were retained in the previous work. This indicates that although retained microsleeper components of the proposed method are in common between subjects, some of these appear to have little discriminative power. Therefore, a feature selection method could potentially improve the prediction performance by selecting the most discriminative common features.

REFERENCES

- [1] R. Jones, G. Poudel, C. Innes, P. R. Davidson, M. Peiris, A. Malla, T. Signal, G. Carroll, R. Watts, and P. Bones, "Lapses of responsiveness: Characteristics, detection, and underlying mechanisms," in *Annu. Int. Conf. IEEE Eng. in Med. and Biol. Soc.*, Aug. 2010, pp. 1788–1791.
- [2] B. C. Tefft, "Prevalence of motor vehicle crashes involving drowsy drivers, United States, 2009–2013," Nov. 2014. [Online]. Available: <https://www.aaafoundation.org/sites/default/files/AAAFoundation-DrowsyDriving-Nov2014.pdf>
- [3] Centre for Road Safety and Transport for NSW, "Road traffic crashes in New South Wales: Statistical statement for the year ended 31 December 2014," 2014. [Online]. Available: <http://roadsafety.transport.nsw.gov.au/downloads/crashstats2014.pdf>
- [4] L. M. Swanson, C. Drake, and J. T. Arnedt, "Employment and drowsy driving: A survey of American workers," *Behav. Sleep Med.*, vol. 10, no. 4, pp. 250–257, 2012.
- [5] W. Vanlaar, H. Simpson, D. Mayhew, and R. Robertson, "Fatigued and drowsy driving: A survey of attitudes, opinions and behaviors," *J. Saf. Res.*, vol. 39, no. 3, pp. 303–309, 2008.
- [6] M. T. R. Peiris, R. D. Jones, P. R. Davidson, G. J. Carroll, and P. J. Bones, "Frequent lapses of responsiveness during an extended visuomotor tracking task in non-sleep-deprived subjects," *J. Sleep Res.*, vol. 15, no. 3, pp. 291–300, 2006.
- [7] G. R. Poudel, C. R. Innes, P. J. Bones, R. Watts, and R. D. Jones, "Losing the struggle to stay awake: Divergent thalamic and cortical activity during microsleeper," *Hum. Brain Mapp.*, vol. 35, no. 1, pp. 257–269, 2014.
- [8] B. Sirois, U. Trutschel, D. Edwards, D. Sommer, and M. Golz, *Predicting accident probability from frequency of microsleeper events*, ser. World Congr. on Med. Phys. and Biomed. Eng. Springer Berlin Heidelberg, 2010, vol. 25/4, pp. 2284–2286.
- [9] S. K. Lal and A. Craig, "Reproducibility of the spectral components of the electroencephalogram during driver fatigue," *Int. J. Psychophysiology*, vol. 55, no. 2, pp. 137–143, 2005.
- [10] Y.-T. Wang, K.-C. Huang, C.-S. Wei, T.-Y. Huang, L.-W. Ko, C.-T. Lin, C.-K. Cheng, and T.-P. Jung, "Developing an EEG based on-line closed-loop lapse detection and mitigation system," *Front. Neurosci.*, vol. 8, no. 321, 2014.
- [11] M. T. R. Peiris, P. R. Davidson, P. J. Bones, and R. D. Jones, "Detection of lapses in responsiveness from the EEG," *J. Neural Eng.*, vol. 8, no. 1, p. 016003, 12 pp, 2011.
- [12] P. Davidson, R. Jones, and M. Peiris, "EEG-based lapse detection with high temporal resolution," *IEEE Trans. Biomed. Eng.*, vol. 54, no. 5, pp. 832–839, May 2007.
- [13] R. Shoorangiz, S. J. Weddell, and R. D. Jones, "Prediction of microsleeper from EEG: Preliminary results," in *38th Annu. Int. Conf. IEEE Eng. in Med. and Biol. Soc.*, Aug 2016, pp. 4650–4653.
- [14] T. Mullen, C. Kothe, Y. Chi, A. Ojeda, T. Kerth, S. Makeig, T.-P. Jung, and G. Cauwenberghs, "Real-time neuroimaging and cognitive monitoring using wearable dry EEG," *IEEE Trans. Biomed. Eng.*, vol. 62, no. 11, pp. 2553–2567, Nov 2015.
- [15] W. D. Clercq, A. Vergult, B. Vanrumste, W. Van Paesschen, and S. Van Huffel, "Canonical correlation analysis applied to remove muscle artifacts from the electroencephalogram," *IEEE Trans. Biomed. Eng.*, vol. 53, no. 12, pp. 2583–2587, Nov 2006.
- [16] J. hua Zhao and P. L. Yu, "A note on variational Bayesian factor analysis," *Neural Networks*, vol. 22, no. 7, pp. 988–997, 2009.
- [17] C. Bishop, *Pattern Recognition and Machine Learning*, ser. Information Science and Statistics. Springer, 2006.